

Influence of layer thickness on the formation of In vacancies in InN grown by molecular beam epitaxy

J. Oila, A. Kemppinen, A. Laakso, and K. Saarinen^{a)}

Laboratory of Physics, Helsinki University of Technology, P.O. Box 1100 FIN-02015 HUT, Finland

W. Egger, L. Liskay,^{b)} and P. Sperr

Institut für Nukleare Festkörperphysik, Universität der Bundeswehr München, D-85577 Neubiberg, Germany

H. Lu and W. J. Schaff

Department of Electrical and Computer Engineering, Cornell University, Ithaca, New York 14853

(Received 26 June 2003; accepted 5 January 2004)

We have used a low-energy positron beam to identify In vacancies in InN layers grown on Al₂O₃ by molecular beam epitaxy. Their concentration decreases from $\sim 5 \times 10^{18}$ to below 10^{16} cm⁻³ with increasing layer thickness (120–800 nm). The decrease in the vacancy concentration coincides with the increase in the electron Hall mobility, suggesting that In vacancies act as electron scattering centers. © 2004 American Institute of Physics. [DOI: 10.1063/1.1651327]

The III-nitride semiconductors, GaN, AlN, and InN, have recently been of a great interest primarily due to their applications in short-wavelength optoelectronic devices. Indium nitride with its band gap of 0.8 eV (Refs. 1 and 2) could extend the wavelength range of III–N materials into the infrared region. The high electron mobility and peak-drift velocity make InN also a promising material for high speed electronics.^{3,4} The fabrication of device-quality InN has, however, failed. The large lattice mismatch with the Al₂O₃ substrate leads to a high density of extended defects. The doping of InN is also a problem. The InN layers are always highly *n* type, possibly due to O_N and Si_{In} impurities, N vacancies, or interstitial hydrogen.^{6,7} Among native defects, N and In vacancies are calculated to have the lowest formation energies, which are, however, predicted to be rather high.⁵

Positron annihilation spectroscopy is based on positron trapping at vacancies due to the missing positive ion core. The trapping can experimentally be observed as increasing positron lifetime and as narrowing of the momentum distribution of annihilating e^+e^- pairs. Our data indicate the presence of In vacancies. The vacancy concentration correlates with the room temperature Hall mobility. This suggests that the vacancies limit the electron mobility, especially in the thinnest layers where their concentration is the highest.

Six InN layers were grown by molecular beam epitaxy (MBE) on Al₂O₃ (0001) substrate, with a 200 nm AlN buffer between the substrate and the InN layer (Table I). In films Nos. 1 and 4 a thin AlN cap was deposited on top of the InN layer. The films are not intentionally doped, but show *n*-type conductivity with the carrier concentrations of $(2-30) \times 10^{18}$ cm⁻³. The electron Hall mobility (300 K) is high, >1100 cm²/V s, in the thickest films, but decreases to below 200 cm²/V s in the thinnest layers.

The positron annihilation experiments were carried out

using a variable energy positron beam. The momentum distribution of the annihilating e^+e^- pairs was determined by measuring the Doppler broadening of the 511 keV annihilation line with a Ge-detector (resolution 1.3 at 511 keV). The low momentum parameter *S* and the high momentum parameter *W*,⁸ describe the shape of the 511-keV line. Positron annihilations with valence electrons increase at a vacancy, increasing the *S* parameter and a decreasing in the *W* parameter. The samples were also characterized using the pulsed positron beam at Universität der Bundeswehr in Munich.⁹ The pulsed beam enables the measurement of the positron lifetime spectrum, $n(t) = \sum I_i \exp(-t/\tau_i)$. Lifetimes τ_i correspond to annihilation of a free positron in the InN lattice and annihilations of positrons trapped at vacancies. Experimentally the positron trapping at vacancies is observed as an increase in the average positron lifetime $\tau_{\text{ave}} = \sum I_i \tau_i$.

Figure 1 shows the *S* parameter measured as a function of the positron beam energy (depth scan). The high *S* parameter observed at low energies ($E < 3$ keV) results from the annihilations at the sample surface and in the thin AlN cap. When the positron energy is increased, fewer positrons can reach the surface and the *S* parameter characteristic to the InN layer can be seen as a constant plateau in the curves. At higher energies the *S* parameter starts to decrease as positrons are able to reach the Al₂O₃ substrate. This turning point in the curves corresponds roughly to the layer thickness, except in sample No. 3 which seems to be thinner than

TABLE I. The thickness, free electron concentration, and electron (Hall) mobility in the studied InN layers. The In vacancy concentration was estimated from positron annihilation measurements.

Sample No.	Thickness (nm)	<i>n</i> (sheet) (10^{14} cm ⁻²)	μ (300 K) (cm ² /V s)	$[V_{\text{In}}]$ (cm ⁻³)
1	120	3.8	175	$\geq 5 \times 10^{18}$
2	200	0.998	657	7×10^{16}
3	270	1.4	616	2×10^{17}
4	380	1.25	753	8×10^{16}
5	600	1.20	1165	$\leq 10^{16}$
6	800	1.7	1113	$\leq 10^{16}$

^{a)}Electronic mail: ksa@fyslab.hut.fi

^{b)}On leave from: KFKI Central Research Institute for Nuclear and Particle Physics, H-1525 Budapest P.O.B. 49, Hungary.

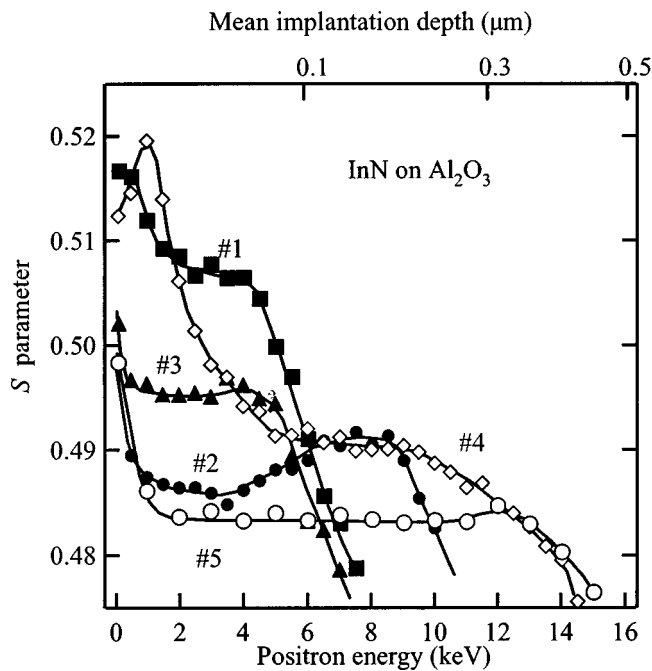


FIG. 1. *S* parameter vs positron beam energy. The corresponding mean implantation depth of positrons is indicated on the top axis.

expected from its nominal thickness (Table I).

The lowest *S* parameter, $S \approx 0.483$ is found in the thickest 600 and 800 nm layers. In the thinner layers the *S* parameter is clearly higher. The increased *S* parameter indicates that positrons get trapped at vacancy defects. In two of the samples (Nos. 2 and 3), the *S* parameter increases towards to the interface, suggesting that the vacancy concentrations are higher in the interface region. The positron lifetime experiments show very similar results. The average positron lifetime τ_{ave} inside the InN layer was 190 ps in the thickest layer (No. 6). In the thinnest layer, where the *S* parameter was also the highest, the average positron lifetime increased up to 260 ps.

The linearity between the parameters *S*, *W*, and τ_{ave} gives information on the number of different positron states.⁸ The (*S*, *W*) plots with positron energy as a running parameter give no indications of positron trapping at the InN/sapphire interfaces. In Fig. 2, the layer-specific *S* and *W* parameters form a line, suggesting that positrons annihilate in two states: as free positrons, characterized by annihilation parameters of defect-free InN (S_b, W_b) and as-trapped at the vacancy (S_v, W_v). Similarly, the dependence between the positron average lifetime and the *S* parameter is linear (Fig. 2), indicating that the vacancy in each of the layers is the same.⁸

Figure 3 shows the high momentum part of the annihilation peak measured using a two-detector (Ge-NaI) coincidence setup to reduce the background level. The results are compared with the theoretical momentum distributions, which were calculated by using atomic core electron wave functions.^{10,11} Above $15 \times 10^{-3} m_0c$ the momentum distribution is mainly made up of the annihilations with the atomic core electrons and it thus gives information on the atoms around the annihilation site. The strongest contribution comes from the 4*d* electrons of indium. At the N vacancy the calculated wave function of positrons overlaps strongly with the neighboring In atoms, resulting in the momentum distri-

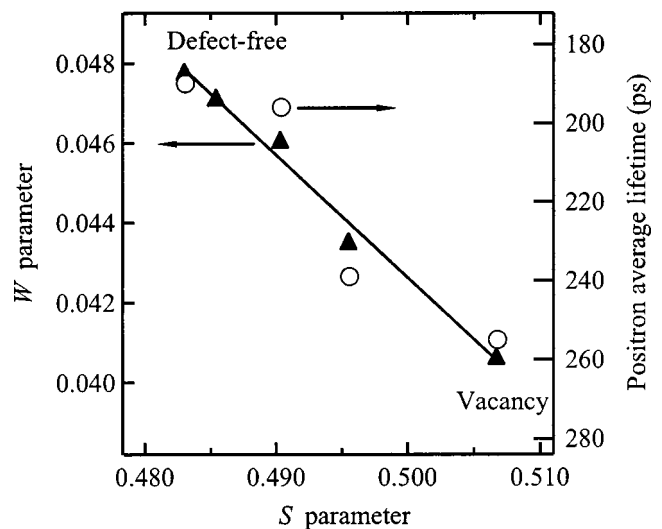


FIG. 2. *S* and *W* parameters and the positron average lifetime in the InN layers. The positron beam energy was chosen to $E=3-7$ keV so that the layer-specific annihilation parameters were recorded. The linearity between the *S* and *W*, and between the *S* and τ_{ave} indicates that the same vacancy is present in all layers.

bution very similar to the free-positron annihilation. In case of the In vacancy, the In atoms are now the second nearest neighbors, which decreases the intensity of the momentum distribution. Such intensity reduction is observed between the samples No. 6 (low vacancy concentration) and No. 1 (high vacancy concentration) which indicates that the observed vacancies are In vacancies.

The identification of the In vacancy is supported also by the positron lifetime experiments. The positron lifetime in a InN lattice was calculated to be 184 ps, and the lifetimes of positrons trapped at N and In vacancies were 186 and 260 ps, respectively. These are close to the experimental

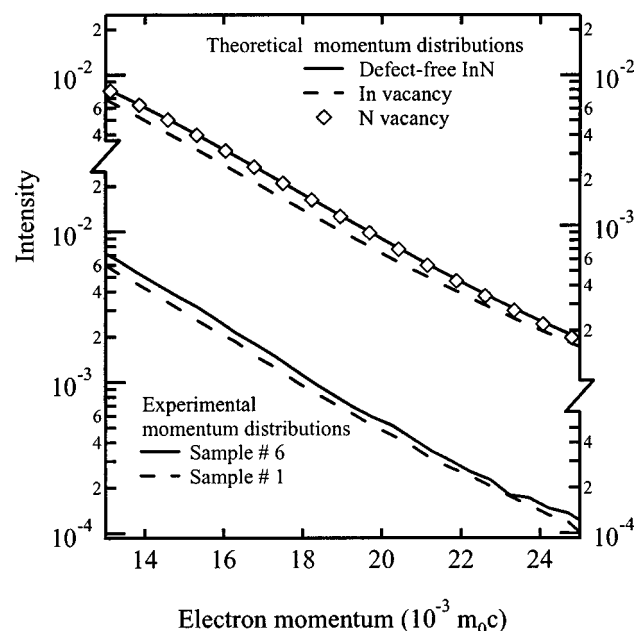


FIG. 3. Core electron momentum distributions in the InN layers. The lower inset presents the experimental results in samples No. 1 and No. 6, measured at beam energies of 2.5 and 7 keV, respectively. The upper inset shows the results of theoretical calculations for the InN lattice and vacancies in both sublattices.

average positron lifetimes of 190 and 260 ps in samples No. 1 and No. 6, respectively (Fig. 2). Although the decomposition of the measured lifetime spectra into free positron and vacancy related components was not successful due to difficulties in the background reduction, the observed difference of about 70 ps between the average positron lifetimes in the thin and thick samples (Fig. 2) can result only from positron trapping at In vacancies.

In the thick layers (Nos. 5 and 6) the parameters S and W remain constant at temperatures 30–300 K, which is typical for free positron annihilation in a lattice. The positron lifetime spectrum measured in the thick layer (No. 6) constitutes mainly of one exponential decay component, also indicating that the vacancy concentration must be very low, $\leq 10^{16} \text{ cm}^{-3}$. The annihilation parameters S_b , W_b , and τ_b recorded in the thickest layers thus represent those of vacancy-free InN.

In the standard positron trapping model the vacancy concentration can be calculated from⁸

$$c_V = \frac{N_{at}}{\mu_V \tau_b} \frac{(S/S_b - 1)}{(S_V/S_b - S/S_b)}, \quad (1)$$

where S_V is the S parameter specific to the vacancy, μ_V the positron trapping coefficient, $N_{at} = 6.367 \times 10^{22} \text{ cm}^{-3}$ is the atomic density, and τ_b the positron lifetime in vacancy free InN. Typically, the S_V parameter for the monovacancy⁸ is about $1.03\text{--}1.05 \times S_b$ (e.g., $S_V \approx 1.046 \times S_b$ for V_{Ga} in GaN^{12}). The S parameter in the thinnest layer (No. 1) is about 4.9% higher than in the thickest layers. The average positron lifetime in the thinnest layer is about the same as the calculated value for the V_{In} . Together these suggest that in the thinnest layer (No. 1) all positrons get trapped at vacancies. The determination of the exact vacancy concentration is not possible, but a lower limit estimate is about $5 \times 10^{18} \text{ cm}^{-3}$.

The vacancy concentrations in other samples (Table I) were estimated by using $\tau_b = 184 \text{ ps}$ and the S parameters recorded in the thickest and thinnest layers as S_b and S_V , respectively. We further take $\mu_V = 2 \times 10^{15} \text{ s}^{-1}$, which is a typical value for negative vacancies.⁸ As a result, the In vacancy concentration decreases over two orders of magnitude when the layer thickness increases (Fig. 4). The higher vacancy concentration closer to the InN/ Al_2O_3 interface is also seen from S and W vs E curves in Fig. 1.

The observation of V_{In} agrees with the theory,⁵ as V_{In} should have the lowest formation energy of all native defects in n -type InN. The higher vacancy concentration closer to the InN/ Al_2O_3 interface suggests that the formation of the vacancies could be related to other defects, e.g., dislocations or impurities, in the interface region. The N vacancy, which has a low formation energy according to theory,⁵ could also be present but escapes detection by positrons due to the positive charge state.

The quality of InN has been shown to increase with the increasing layer thickness.^{13,14} This is evident also in this study, where the Hall mobility increases from below 200 to above $1100 \text{ cm}^2/\text{V s}$ as the layer thickness is increased (Fig. 4). The enhanced electron mobility indicates that the defect

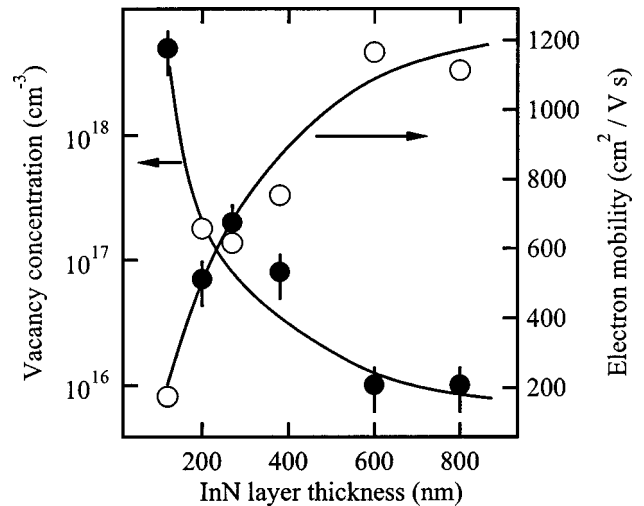


FIG. 4. Electron Hall mobility and In vacancy concentration as a function of the InN layer thickness.

densities are reduced at longer distances from the interface. The vacancy concentration simultaneously decreases drastically (Fig. 4), suggesting that the observed vacancies limit the electron mobility by acting as scattering centers.

In summary, we observe In vacancies in MBE-grown InN layers by positron annihilation spectroscopy. The concentration of vacancies decreases with the increasing layer thickness. The decrease in $[V_{\text{In}}]$ from above 10^{18} to below 10^{16} cm^{-3} correlates with the increase in the electron Hall mobility, suggesting that the vacancies may significantly limit the electron mobility in the thinner layers.

The work has been partly financed by the Academy of Finland (DENOS Project). The authors also acknowledge the support of Colin Wood at the Office of Naval Research.

- ¹V. Yu. Davydov, A. A. Klochikhin, R. P. Seisyan, V. V. Emtsev, S. V. Ivanov, F. Bechstedt, J. Furthmüller, H. Harima, A. V. Mudryi, J. Aderhold, O. Semchinova, and J. Graul, *Phys. Status Solidi B* **229**, R1 (2002).
- ²J. Wu, W. Walukiewicz, K. M. Yu, J. W. Ager III, E. E. Haller, H. Lu, W. J. Schaff, Y. Saito, and Y. Nanishi, *Appl. Phys. Lett.* **80**, 3967 (2002).
- ³E. B. Bellotti, B. K. Doshi, K. F. Brennan, J. D. Albrecht, and P. P. Ruden, *J. Appl. Phys.* **85**, 916 (1999).
- ⁴B. E. Foutz, S. K. Leary, M. S. Shur, and L. F. Eastman, *J. Appl. Phys.* **85**, 7727 (1999).
- ⁵C. Stampfl, C. G. Van de Walle, D. Vogel, P. Krüger, and J. Pollmann, *Phys. Rev. B* **61**, R7846 (2000).
- ⁶D. C. Look, H. Lu, W. J. Schaff, J. Jasinski, and Z. Liliental-Weber, *Appl. Phys. Lett.* **80**, 258 (2002).
- ⁷E. A. Davis, S. F. J. Cox, R. L. Lichti, and C. G. Van de Walle, *Appl. Phys. Lett.* **82**, 592 (2003).
- ⁸K. Saarinen, P. Hautojärvi, and C. Corbel, in *Identification of Defects in Semiconductors*, edited by M. Stavola (Academic, New York, 1998), p. 209.
- ⁹W. Bauer-Kugelmann, P. Sperr, G. Kögel, and W. Triftshäuser, *Mater. Sci. Forum* **363–365**, 529 (2001).
- ¹⁰M. Alatalo, H. Kauppinen, K. Saarinen, M. J. Puska, J. Mäkinen, P. Hautojärvi, and R. M. Nieminen, *Phys. Rev. B* **51**, 4176 (1995).
- ¹¹M. Alatalo, B. Barbiellini, M. Hakala, H. Kauppinen, T. Korhonen, M. J. Puska, K. Saarinen, P. Hautojärvi, and R. M. Nieminen, *Phys. Rev. B* **54**, 2397 (1996).
- ¹²K. Saarinen, P. Seppälä, J. Oila, P. Hautojärvi, C. Corbel, O. Briot, and R. L. Aulombard, *Appl. Phys. Lett.* **73**, 3253 (1998).
- ¹³S. Yamaguchi, M. Kariya, S. Nitta, T. Takeuchi, C. Wetzel, H. Amano, and I. Akasaki, *J. Appl. Phys.* **85**, 7682 (1999).
- ¹⁴H. Lu, W. J. Schaff, J. Hwang, H. Wu, G. Koley, and L. F. Eastman, *Appl. Phys. Lett.* **79**, 1489 (2001).